Distorted-wave-approximation cross sections for excitation of the $b\,^3\Sigma_u^+$ and $B\,^1\Sigma_u^+$ states of H_2 by low-energy-electron impact

Arne W. Fliflet and Vincent McKoy

Arthur Amos Noyes Laboratory of Chemical Physics, California Institute of Technology, Pasadena, California 91125*

(Received 15 January 1979)

Distorted-wave-approximation calculations are reported for the excitation of the $b\,^3\Sigma_u^+$ and $B\,^1\Sigma_u^+$ states of H_2 by electron impact. A discrete-basis-set method is used to obtain the electron-molecule continuum wave functions. Differential and integrated cross sections are presented from near threshold up to 60-eV electron impact energy. Comparison is made with other theoretical results and experimental data.

I. INTRODUCTION

Electronic excitation of molecules by low-energy electron impact is an important process in gas laser systems and other weakly ionized plasmas. *Ab initio* theoretical methods are clearly of interest, but the development of accurate methods has been slow primarily owing to the difficulty of calculating wave functions for the highly nonspherical electron-molecule interaction potential. Most calculations to date for electronic excitation have made use of some form of the Born approximation, which is reliable only at high impact energies and small scattering angles. Calculations for inelastic electron scattering from light atoms have recently been reviewed by Bransden and McDowell.[1] These calculations indicate that distorted-wave methods have considerable utility in the intermediate energy region extending from the ionization threshold up to several hundred eV. Distorted-wave methods are much easier to apply than close-coupling methods and thus seem well suited to the study of electronically inelastic electron-molecule scattering.

In this study of the excitation of the first singlet and triplet excited states of H_2 by low-energy electron impact, we use a distorted-wave prescription first applied to e^--H_2 scattering by Rescigno, McCurdy, McKoy, and Bender.[2] As shown by Rescigno, McCurdy, and McKoy,[3] this prescription is equivalent to the "first-order many-body theory" (FOMBT) of Taylor and coworkers.[4] A simplifying feature of this model is that both the incoming and outgoing distorted-wave functions are calculated in the field of the target ground state. Thomas *et al.*[5] have applied the FOMBT to the excitation of several excited states of He. Their results are generally in good agreement with experiment for spin-allowed transitions, while for spin-forbidden transitions the FOMBT often overestimates the total cross section by a factor of 3 or 4, although the general shape of the differential cross section may be reproduced.

In a recent paper we presented a discrete-basis-set method for calculating electron-molecule continuum functions.[6] The method is a development of the T-matrix approach to electron-molecule scattering introduced by Rescigno, McCurdy, and McKoy.[7] In this work we use this method to calculate distorted-wave functions in the static-exchange approximation. Our technique allows us to treat spin-allowed excitation processes where the transition potential has long-range moments.

The theory of angular distributions of collision products expressed in terms of the angular momentum $\vec{j}_t$ transferred during the collision has been discussed by Fano and Dill.[8] In this representation the differential cross section is given by an incoherent sum of contributions corresponding to different magnitudes of $\vec{j}_t$. As pointed out recently by Siegel, Dill, and Dehmer,[9] use of the j_t representation simplifies the averaging with respect to target rotational quantum numbers in electron-molecule scattering. This simplification is especially valuable in the treatment of electron impact excitation of spin-allowed electronic transitions since this process may be dominated by high-angular-momentum scattering. In this case a single-center expansion of the scattering amplitude in terms of $\vec{j}_t$ converges much more rapidly than the usual expansion in terms of the incident-electron angular momentum. In this work we also make use of the fact that in the j_t representation the Born approximation to the scattering amplitude for electronic excitation can be evaluated in closed form when the target molecular orbitals are expanded in terms of Cartesian Gaussian functions. The derivation of expressions for a linear target molecule is outlined in the Appendix.

Excitation of the $B\,^1\Sigma_u^+$ state of H_2 is of particular interest as a test of theory because absolute experimental data has recently been obtained by Srivastava and Jensen.[10] The integrated cross sections for excitation of this state and several triplet states of H_2 have been calculcated in the two-state close-coupling approximation by

Chung and Lin.[11] Their results for the $B\ ^1\Sigma_u^+$ state are about a factor of two larger than the experimental data of Srivastava and Jensen.[10] Our differential cross sections for excitation of the $B\ ^1\Sigma_u^+$ are in good qualitative agreement with the experimental data. However, our integrated cross section agrees with the results of Chung and Lin.[11]

Our results for the dissociative $b\ ^3\Sigma_u^+$ state are in good agreement with the distorted-wave results of Rescigno *et al.*[2] as expected, and we have obtained results for impact energies up to 60 eV. Our peak integrated cross section for this state is about a factor of three larger than Chung and Lin's two-state close-coupling result[11]; however, near threshold our results are in good agreement with Corrigan's dissociation data.[12] The applicability of the distorted-wave approximation—which does not account for resonance effects—in the threshold region is discussed in Section IV. At impact energies of 40-eV and above, our differential cross sections for the $b\ ^3\Sigma_u^+$ state are in qualitative agreement with the angular distribution data of Trajmar *et al.*[13]

II. THEORY

In the Born-Oppenheimer approximation, the electronic part of the electron-molecule scattering wave function satisfies the fixed-nuclei Schrödinger equation

$$(-\tfrac{1}{2}\nabla^2 + V_{\text{int}} - \tfrac{1}{2}k^2)\Psi_{\vec{k}_0}(R;\vec{x},\vec{x}_1,\ldots,\vec{x}_N) = 0\,, \tag{1}$$

where

$$V_{\text{int}} = -\frac{Z_A}{|\vec{r}-\vec{R}_A|} - \frac{Z_B}{|\vec{r}-\vec{R}_B|} + \sum_{j=1}^{n}\frac{1}{|\vec{r}-\vec{r}_j|} \tag{2}$$

for a diatomic molecule. The incident-electron momentum is denoted by $\vec{k}_0$; the parametric dependence of the elctronic wave function on the internuclear separation is denoted by $R = |\vec{R}_A - \vec{R}_B|$; $\vec{x}$, $\vec{x}_i$, $i=1$ to N denote the combined space and spin coordinates of the scattered and target electrons, space coordinates alone are denoted by $\vec{r}, \vec{r}_i$; N is the number of target electrons; and Z_A, Z_B are the nuclear charges. Except as noted, we use atomic units throughout. The scattering wave function has the asymptotic form

$$\Psi_{\vec{k}_0} \to e^{i\vec{k}_0\cdot\vec{r}}\chi_0(s)\Phi_0(\vec{x}_1,\ldots,\vec{x}_N) + \sum_n f_{\vec{k}_0}(n\leftarrow 0;R,\hat{r})(e^{ik_n r}/r)\chi_n(s)\Phi_n(\vec{x}_1,\ldots,\vec{x}_N) \tag{3}$$

as $r\to\infty$, where Φ_0, Φ_n are the initial, final target wave functions; $\chi_0(s), \chi_n(s)$ are the initial, final spin wave functions of the scattered electron; and

$$\tfrac{1}{2}k_n^2 = \tfrac{1}{2}k_0^2 - (E_n - E_0)\,, \tag{4}$$

where E_0, E_n are the initial, final target-state energies. The body-framed fixed nuclei scattering amplitude is related to the electronic portion of the transition matrix according to

$$f_{\vec{k}_0}(n\leftarrow 0;R,\hat{r}) = -2\pi^2\langle\vec{k}_n, n\,|T_{\text{el}}|\,\vec{k}_0, 0\rangle\,, \tag{5}$$

where $\hat{k}_n = \hat{r}$.

In the prescription for inelastic scattering proposed by Rescigno *et al.*,[3] the scattering is treated in a form of the distorted-wave (DW) approximation derived from the two-potential formula[14]; the initial target state is the Hartree-Fock ground state; and the final target state is treated in the random-phase approximation (RPA).[15] A notable feature of this formulation is that both the initial and final distorted-wave functions are calculated in the static-exchange potential of the ground state.

In the present calculation we follow the prescription of Rescigno *et al.*[3] except that the final target state is treated in the single-channel Tamm-Dancoff approximation (TDA).[14] The single-channel TDA is equivalent to an independent-electron picture in which the excited orbital is an eigenfunction of the V^{N-1} potential.[16] In our formulation the electronic portion of the transition matrix element involves matrix elements of the form

$$\langle\vec{k}_n, n\,|T_{\text{el}}|\,\vec{k}_0, 0\rangle = \langle\bar{\phi}_n\psi_{\vec{k}_n}^{(-)}\,|v\,|\phi_\alpha\psi_{\vec{k}_0}^{(+)}\rangle_a\,, \tag{6}$$

where $\psi_{\vec{k}_0}^{(+)}, \psi_{\vec{k}_n}^{(-)}$ are the initial, final Hartree-Fock (static-exchange) continuum spin-orbitals satisfying outgoing-wave, incoming-wave boundary conditions; ϕ_α is the Hartree-Fock occupied spin orbital; and $\bar{\phi}_n$ is a spin orbital of the V^{N-1} potential formed by removing an electron from the target orbital α. The antisymmetrized matrix element is defined as

$$\langle ij\,|v\,|kl\rangle_a = \langle ij\,|v\,|kl\rangle - \langle ij\,|v\,|lk\rangle\,, \tag{7}$$

where

$$\langle ij\,|v\,|kl\rangle = \int d\vec{x}_1\, d\vec{x}_2\, \phi_i^*(\vec{x}_1)\phi_j^*(\vec{x}_2) \times (1/|\vec{r}_1 - \vec{r}_2|)\phi_k(\vec{x}_1)\phi_l(\vec{x}_2)\,. \tag{8}$$

To treat the target orientation dependence of the scattering analytically, it is convenient to expand the initial and final continuum space orbitals in the partial-wave series:

$$\psi_{\vec{k}_0}^{(+)}(\vec{r}) = \left(\frac{2}{\pi}\right)^{1/2}\sum_{lm} i^l\psi_{k_0 lm}^{(+)}(\vec{r})Y_{lm}(\hat{k}_0)\,, \tag{9a}$$

$$\psi_{\vec{k}_n}^{(-)}(\vec{r}) = \left(\frac{2}{\pi}\right)^{1/2}\sum_{lm} i^l\psi_{k_n lm}^{(-)}(\vec{r})Y_{lm}(\hat{k}_n)\,. \tag{9b}$$

This leads to a single-center expansion of the electronic portion of the transition matrix of the form

$$\langle \mathrm{k}_n, n | T_{\mathrm{el}} | \mathrm{k}_0, 0\rangle = \sum_{ll'mm'} i^{l'-l} \times \langle k_n lm, n | T_{\mathrm{el}} | k_0 l'm', 0\rangle \times Y_{lm}(\hat{k}_n) Y^*_{l'm'}(\hat{k}_0) . \quad (10)$$

Similarly, the fixed nuclei scattering amplitude in the body-fixed frame has the expansion

$$f_{\vec{k}_0}(n \leftarrow 0; R, \hat{r}) = 4\pi \sum_{ll'mm'} f_{ll'mm'}(n \leftarrow 0; R, k_0) Y_{lm}(\hat{r}) Y^*_{l'm'}(\hat{k}_0) \quad (11)$$

(recalling that $\hat{k}_n = \hat{r}$). We now relate the body-fixed-frame scattering amplitude to the scattering amplitude in the laboratory frame, denoted by primed coordinates and defined with z' axis in the direction of incident momentum. Using the properties of spherical harmonics and introducing the rotational harmonics defined by Edmonds,[17] we obtain

$$f_{\vec{k}_0}(n \leftarrow 0; \vec{R}', \hat{r}') = 4\pi \sum_{ll'mm'm''} \left(\frac{2l'+1}{4\pi}\right)^{1/2} f_{ll'mm'}(n \leftarrow 0; R, k_0) \times D^{(l)}_{m''m}(\hat{R}') D^{(l')*}_{om'}(\hat{R}') Y_{lm''}(\hat{r}') , \quad (12)$$

where $\vec{R}'$ specifies target orientation and internuclear separation, and $\hat{r}'$ denotes the scattering angles in the laboratory frame. Following Temkin *et al.*,[18] we express the laboratory-frame scattering amplitude in terms of fixed-nuclei dynamical coefficients:

$$f_{k_0}(n \leftarrow 0; \vec{R}, \hat{r}') = \sum_{ll'mm'm''} a_{ll'mm'}(n \leftarrow 0; k_0, R) \times D^{(l')*}_{m'm}(\hat{R}') D^{(l')}_{om'}(\hat{R}') Y_{lm''}(\hat{r}') . \quad (13)$$

Comparing Eqs. (12) and (13), and using Eqs. (5), (10), and (11), we obtain

$$a_{ll'mm'}(n \leftarrow 0; k_0, R) = -\tfrac{1}{2}\pi [4\pi(2l'+1)]^{1/2} i^{l'-l} \times \langle k_n lm, n | T_{\mathrm{el}} | k_0 l'm', 0\rangle . \quad (14)$$

To account for the motion of the target nuclei we use the adiabatic nuclei approximation[19]

$$f_{k_0}(n\upsilon_n j_n \leftarrow 0\upsilon_0 j_0; \hat{r}') = \langle \Theta^n_{\upsilon_n j_n}(\vec{R}') | f_{k_0}(n \leftarrow 0; \vec{R}', \hat{r}') | \Theta^0_{\upsilon_0 j_0}(\vec{R}')\rangle , \quad (15)$$

where $\Theta^n_{\upsilon_n j_n}, \Theta^0_{\upsilon_0 j_0}$ are the final and initial target nuclear wave functions. This approximation is valid when the speed of the scattered electron is fast compared to the motion of the target nuclei.

As a further simplification we neglect the dependence of the fixed-nuclei scattering amplitude on internuclear separation. The electronic part of the transition matrix is then calculated only at the equilibrium internuclear separation and the probability for transitions between initial and final vibrational states is given by the Franck-Condon factor

$$q_{\upsilon_n\upsilon_0} = \left| \int dR\, R^2\, \zeta^{n*}_{\upsilon_n}(R) \zeta^0_{\upsilon_0}(R) \right|^2 , \quad (16)$$

where $\zeta^n_{\upsilon_n}$, $\zeta^0_{\upsilon_0}$ are the initial and final target vibrational wave functions.

Finally, we neglect the dependence of the scattering amplitude on final vibrational quantum numbers. A single electronic transition matrix element is calculated with outgoing electron energy determined by the vertical transition energy from the $\upsilon = 0$ ground state to the final vibrational level with the largest Franck-Condon factor. Assuming the target rotational levels are essentially degenerate, we obtain the rotationally averaged cross section by averaging the fixed-nuclei cross section with respect to orientation. Averaging over initial and summing over final spin states then leads to the following expression for the differential cross section for exciting a vibrational level of an electronically excited target state:

$$\frac{d\sigma}{d\Omega'}(n\upsilon_n \leftarrow 0\upsilon_0) = \tfrac{1}{2}(2S+1)\frac{k_{\upsilon_n}}{k_0} q_{\upsilon_n\upsilon_0} \frac{1}{8\pi^2} \times \int d\hat{R}' \left| f_{k_0}(n \leftarrow 0; \hat{R}', \hat{r}') \right|^2 , \quad (17)$$

where S is 0 or 1 for the excitation of a singlet state or triplet state, respectively, from a singlet ground state. To obtain the differential cross section summed over final vibrational level the factor $k_{\upsilon_n} q_{\upsilon_n\upsilon_0}$ is replaced by $\sum_{\upsilon_n} k_{\upsilon_n} q_{\upsilon_n\upsilon_0}$.

To carry out the averaging with respect to target orientation we use two different methods depending on the transition involved. For singlet-triplet transitions the single-center expansion of the scattering amplitude converges rapidly. In this case a convenient expression for the differential cross section is obtained by substituting Eq. (13) directly into Eq. (17). Carrying out the angular integration we obtain

$$\frac{d\sigma}{d\Omega'}(n\nu_n \leftarrow 0\nu_0) = S\frac{k_{\nu_n}}{k_0} q_{\nu_n\nu_0} \sum_L A_L P_L(\theta') , \quad (18)$$

where

$$A_L = \frac{1}{4\pi} \sum_{\substack{ll'mm' \\ \lambda\lambda'\mu\mu'}} a_{ll'mm'} a^*_{\lambda\lambda'\mu\mu'} \frac{2L+1}{2\lambda'+1} \left(\frac{2l+1}{2\lambda'+1}\right)^{1/2} \times (Ll00|\lambda 0)(Ll'00|\lambda' 0)(Ll\mu - m, m|\lambda\mu) \times (Ll', -\mu' + m', -m'|\lambda', -\mu') . \quad (19)$$

The symbol $(l_1 l_2 m_1 m_2 | l_3 m_3)$ denotes a Clebsch-Gordan coefficient; $P_2(\theta')$ is a Legendre polynomial. The transition potential for singlet-singlet transitions generally has long-range moments which lead to scattering by high-angular-momentum electrons. In this case the single-center expansion for the scattering given in Eq. (13) converges slowly and evaluation of the coherent sum in Eq. (19) is computationally inefficient.

Siegel, Dill, and Dehmer[9] have pointed out that it is advantageous to transform to the so-called j_t basis in which components of the scattering amplitude are classified by the angular momentum transferred during the collision,

$$\vec{j}_t = \vec{l} - \vec{l}' . \tag{20}$$

The single-center expansion of the scattering amplitude is then of the form

$$f_{k_0}(n \leftarrow 0; \vec{R}', \vec{r}') = \sum_{j_t m_t m_t'} B^{j_t}_{m_t m_t'}(n \leftarrow 0; k_0 R', \hat{r}') D^{(j_t)}_{m_t m_t'}(\hat{R}') , \tag{21}$$

where

$$B^{j_t}_{m_t m_t'}(n \leftarrow 0; k_0, R', \hat{r}') = \frac{2j_t + 1}{8\pi^2} \int d\hat{R}' \, D^{(j_t)}_{m_t m_t'}(\hat{R}') f_{k0}(n \leftarrow 0; \vec{R}', \hat{r}') . \tag{22}$$

The z component of $\vec{j}_t$ in the lab frame is given by m_t, and in the body-fixed frame by m_t'. Substitution of Eq. (21) into Eq. (17) leads to an *incoherent* sum for the differential cross section

$$\frac{d\sigma}{d\hat{\Omega}'}(n\nu_n \leftarrow 0\nu_0) = \tfrac{1}{2}(2S+1)\frac{k_{\nu_n}}{k_0} q_{\nu_n \nu_0} \sum_{j_t, m_t, m_t'} \frac{1}{2j_t + 1} \times |B^{j_t}_{m_t m_t'}(n \leftarrow 0; k_0, R', \Omega')|^2 . \tag{23}$$

For a linear molecule m_t' is determined by the electronic transition. The sum over j_t and m_t in Eq. (23) converges rapidly even when the transition potential has long-range moments. Substitution of Eq. (13) into Eq. (22) yields an expression for the j_t- basis expansion coefficients in terms of the fixed-nuclei dynamical coefficients:

$$B^{j_t}_{m_t m_t'}(\Omega') = \sum_{l l' m m'} (-1)^{m'} a_{l l' m m'} (l' l 0 m_t | j_t m_t) \times (l' l, -m', m | j_t m_t') Y_{l m_t}(\hat{\Omega}') . \tag{24}$$

For sufficiently high angular momenta exchange effects become small and the projectile is scattered mostly at small angles by the long-range moments of the transition potential. In this range the fixed-nuclei dynamical coefficients are adequately represented by the first Born approximation (BA). The number of dynamical coefficients needed to converge the right-hand side of Eq. (24) can therefore be significantly reduced by rewriting Eq. (24) as follows:

$$B^{j_t}_{m_t m_t'}(\hat{\Omega}') = B^{j_t (\mathrm{BA})}_{m_t m_t'}(\hat{\Omega}') + \Delta B^{j_t, L}_{m_t m_t'}(\hat{\Omega}') , \tag{25}$$

where

$$\Delta B^{j_t, L}_{m_t m_t'}(\hat{\Omega}') = \sum_{l l' m m'}^{L} (a_{l l' m m'} - a^{(\mathrm{BA})}_{l l' m m'}) (l' l 0 m_t | j_t m_t) \times (l' l, -m', m | j_t m_t') Y_{l m_t}(\hat{\Omega}') . \tag{26}$$

The symbol L denotes a set of indices $(ll'mm')$ such that, for larger values of any index, $a_{ll'mm'} \approx a^{(\mathrm{BA})}_{ll'mm'}$.

If the target electronic orbitals are expanded in terms of Cartesian Gaussian functions, the BA j_t-basis expansion coefficients $B^{j_t (\mathrm{BA})}_{m_t m_t'}(\hat{\Omega}')$ can be expressed in closed form for a general polyatomic molecule. The derivation of formulas valid for a linear molecule is outlined in the Appendix.

To obtain a representation of the continuum-space orbital, we use a method discussed previously[6] based on the discrete-basis-set T-matrix method introduced by Rescigno, McCurdy, and McKoy.[7] In this approach the scattering potential is approximated by its projection onto a subspace of square-integrable functions

$$U^t = \sum_{\alpha\beta} |\alpha\rangle\langle\alpha|U|\beta\rangle\langle\beta| . \tag{27}$$

For potentials of this form the Lippmann-Schwinger equation for the T matrix

$$T = U + U G_0^+ T , \tag{28}$$

where G_0^+ is the free-particle Green's function for the outgoing-wave boundary condition, reduces to a finite matrix equation with solution

$$T^t = (1 - U^t G_0^+)^{-1} U^t . \tag{29}$$

It is convenient to work with the K matrix which satisfies the Lippmann-Schwinger equation

$$K = U + U G_0^{\mathrm{P}} K , \tag{30}$$

where G_0^{P} is the principal-value part of G_0^+. The K-matrix solution

$$K^t = (1 - U^t G_0^{\mathrm{P}})^{-1} U^t \tag{31}$$

corresponds to the wave function

$$\psi^t_{klm} = \phi_{klm} + G_0^{\mathrm{P}} K^t \phi_{klm} , \tag{32}$$

where $\phi_{klm} = j_k(kr) Y_{lm}(\hat{r})$ and $j_l(kr)$ is a spherical Bessel function. The wave function ψ^t_{klm} satisfies the Schrödinger equation

$$(-\nabla^2 + U^t - k^2)\psi^t_{klm} = 0 . \tag{33}$$

Introducing the single-center expansion

$$\psi^t_{klm}(\mathbf{r}) = \sum_{l'} g^t_{ll'm}(k,r) Y_{l'm}(\hat{r}) , \tag{34}$$

the asymptotic behavior of ψ^t_{klm} is given by

$$\psi^t_{klm} \to \sum_{l'} [j_{l'}(kr)\delta_{ll'} - y_{l'}(kr)\langle kl'm|K^t|klm\rangle] Y_{l'm}(\hat{r}) \tag{35}$$

as $r \to \infty$, where $y_{l'}(kr)$ is an irregular spherical Bessel function. To obtain a numerical representation of ψ^t_{klm} we substitute the identity

$$K^t \phi_{klm} = U^t \psi^t_{klm} \tag{36}$$

into Eq. (33) and make use of the single-center expansion Eq. (34). This leads to a set of *uncoupled* differential equations for the radial functions $g^t_{ll'm}$ of the form

$$\left(-\frac{d^2}{dr^2} + \frac{l'(l'+1)}{r^2} - k^2\right) r g^t_{ll'm}(k,r) = -r\langle Y_{l'm}|K^t|klm\rangle . \tag{37}$$

A technique for solving this equation subject to the boundary conditions:

$$\lim_{r\to 0} r g^t_{ll'm}(k,r) = 0 \tag{38}$$

and

$$g^t_{ll'm}(k,r) \to j_{l'}\delta_{ll'} - y_{l'}\langle kl'm|K^t|klm\rangle \tag{39}$$

as $r \to \infty$, is given in Ref. 6. Traveling-wave boundary-condition wave functions are obtained from the standing-wave solution by the transformation[20]

$$\psi^{(\pm)}_{klm} = \sum_{l'} (1 \mp iK)^{-1}_{ll'} \psi^t_{kl'm} . \tag{40}$$

It is convenient to express the electronic portion of the transition matrix in terms of a nonlocal transition potential

$$U_{no} = U^d_{no} + U^{ex}_{no} , \tag{41}$$

where U^d_{no} is the direct (local) part and U^{ex}_{no} is the exchange (nonlocal) part. In singlet-to-triplet-state excitation processes, only the exchange part contributes. The transition potential is defined by the equation

$$\langle k_n lm, n|T_{el}|k_0 l'm';0\rangle = \langle \psi^{(-)}_{k_n lm}|U_{no}|\psi^{(+)}_{k_0 l'm'}\rangle . \tag{42}$$

Substituting Eq. (40) in Eq. (42) and using the approximate continuum wave functions discussed above leads to

$$\langle k_n lm, n|T_{el}|k_0 l'm', 0\rangle \cong \sum_{l'',l'''} (1 - iK^t)^{-1}_{ll''m} \times \langle \psi^t_{k_n l''m}|U_{no}|\psi^t_{k_0 l'''m'}\rangle \times (1 - iK^t)_{l'''l'm'} , \tag{43}$$

where $K^t_{ll'm} = \langle klm|K^t|kl'm\rangle$. To calculate $\langle \psi^t_{k_n lm}|U_{no}|\psi^t_{k_0 l'm'}\rangle$ we use the single-center expansion method discussed in previous work.[6,21] The method involves single-center expansions for the Coulomb interaction

$$\frac{1}{|\vec{r} - \vec{r}'|} = \sum_{\lambda=0}^{\infty} \frac{r_<^\lambda}{r_>^{\lambda+1}} P_\lambda(\hat{r}\cdot\hat{r}') , \tag{44}$$

the target orbitals

$$\phi_\sigma(\vec{r}) = \sum_{s=0}^{\infty} \phi^\sigma_{sm_\sigma}(r) Y_{sm_s}(\hat{r}) , \tag{45}$$

and the continuum orbitals. For spin-allowed transitions, we calculate the multipole moments of the direct transition potential

$$U^d_{no}(\vec{r}) = 2\sum_{\lambda m_\lambda} V^{no}_{\lambda m_\lambda} Y_{\lambda m_\lambda}(\vec{r}) , \tag{46}$$

where

$$V^{no}_{\lambda m_\lambda} = N_\alpha (-1)^{m_\alpha} \sum_{ss'} \frac{[(2s+1)(2s'+1)]^{1/2}}{2\lambda+1} \times (ss', -m_\alpha, m_n|\lambda m_\lambda)(ss'00|\lambda 0) \times \left\langle \phi^\alpha_{sm_\alpha}\left|\frac{r_<^\lambda}{r_>^{\lambda+1}}\right|\bar{\phi}^n_{s'm_n}\right\rangle \tag{47}$$

and

$$\left\langle \phi^\alpha_{sm_\alpha}\left|\frac{r_<^\lambda}{r_>^{\lambda+1}}\right|\bar{\phi}^n_{s'm_n}\right\rangle = \frac{1}{r^{\lambda+1}}\int_0^r dr' r'^2 \phi^\alpha_{sm_\alpha}(r')\bar{\phi}^n_{s'm_n}(r') r'^\lambda + r^\lambda \int_r^\infty dr' r'^2 \phi^\alpha_{sm_\alpha}(r')\bar{\phi}^n_{s'm_n}(r') r'^{-\lambda-1} . \tag{48}$$

These and the following expressions for U_{no} assume an axially symmetric target; N_α is the occupation number of the subshell α. Matrix elements of the direct transition potential are given by the expansion

$$\langle \psi^t_{k_n lm}|U^d_{no}|\psi^t_{k_0 l'm'}\rangle = 2\left(\frac{2l+1}{2l'+1}\right)^{1/2} \sum_{s,s',\lambda,m_\lambda} (s\lambda 00|s'0)(s\lambda m m_\lambda|s'm') \times \int_0^\infty dr\, r^2 g^t_{lsm}(k_n, r) V^{no}_{\lambda m_\lambda}(r) g^t_{l's'm'}(k_0, r) . \tag{49}$$

The matrix element of the exchange transition

potential has an expression of the form

$$\langle \psi^t_{k_n lm} | U^{ex}_{no} | \psi^t_{k_0 l'm'} \rangle = \sum_{\substack{l'' l''' \\ ss'\lambda}} A(l'', m; l''', m'; s, m_n; s' m_\alpha; \lambda) \times R^\lambda(g^t_{ll''m}, \bar{\phi}^n_{sm_n}; \phi^\alpha_{s'm_\alpha}, g^t_{l'l'''m'}), \quad (50)$$

where

$$A(l'', m; l''', m'; s, m_n; s' m_\alpha; \lambda) = \left(\frac{(2s+1)(2s'+1)}{(2l''+1)(2l'''+1)}\right)^{1/2} (s\lambda 00 | l''0)(s'\lambda 00 | l''0) \times (s\lambda m_n, m' - m_n | l'''m')(s'\lambda m_\alpha, m - m_\alpha | l''m) \quad (51)$$

and

$$R^\lambda(\phi_1, \phi_2; \phi_3, \phi_4) = \int_0^\infty dr\, r^2 \phi_1^*(r)\phi_3(r)\left(r^{-\lambda-1}\int_0^r dr'\, r'^2 \phi_2^*(r')\phi_4(r')r'^\lambda + r^\lambda \int_r^\infty dr'\, r'^2 \phi_2^*(r')\phi_4(r')r'^{-\lambda-1}\right). \quad (52)$$

III. CALCULATIONS AND RESULTS

For the wave function for the ground state of H_2, we carried out a self-consistent-field (SCF) calculation at an internuclear spacing of 1.4006 a.u. The SCF basis consists of a $(10s5p_z)$ set of primitive Gaussians on each nuclear center contracted to $(7s5p_z)$. The Huzinaga exponents and contraction coefficients for this basis set are given in Ref. 6. The $b\ ^3\Sigma_u^+$ and $B\ ^1\Sigma_u^+$ states of H_2 have the electronic configuration $\sigma_g\bar{\sigma}_u$, where $\bar{\sigma}_u$ is the appropriate σ_u eigenfunction of the V^{N-1} potential. We solved for thse orbitals in a basis of Cartesian Gaussian functions using the computer codes developed by Goddard and coworkers.[22] We used the same basis set for the diagonalization of the V^{N-1} potential as for the SCF calculation. The vertical excitation energies for the $b\ ^3\Sigma_u^+$ and $B\ ^1\Sigma_u^+$ states of H_2 in this basis set are 9.70 and 12.51 eV, respectively, from the $v=0$ ground-state vibrational level to the excited-state potential curve. These values agree well with the corresponding transition energies of 10.14 and 12.48 eV obtained by using the potential-energy curves of Kolos and Wolniewicz.[23] We used the latter values to determine the energy of the outgoing electron via Eq. (4) for the electronic transition matrix element.

Our prescription for computing the distorted-wave matrix element $\langle \psi^t_{k_n lm} | U_{no} | \psi^t_{k_0 l'm} \rangle$ involves single-center expansions for the continuum wavefunctions, the target orbitals, and the direct transition potential. We obtain convergence of the distorted-wave matrix elements to three significant figures by including $l' \leq 11$ in the single-center expansion [Eq. (36)] of ψ^t_{klm}, $s \leq 11$ in the expansion [Eq. (44)] of ϕ_σ, and $\lambda \leq 11$ in the expansion [Eq. (45)] of U^d_{no}. The radial one- and two-electron integrals occurring in Eqs. (46), (48), and (49) are evaluated by Simpson's Rule quadrature.

Our technique for computing numerical representations of the continuum radial orbitals $g^t_{ll'm}$ occurring in the single-center expansion of ψ^t_{klm} is described in Ref. 6. The Gaussian basis sets used to construct U^t are given in Ref. 21 [Table I B for σ-symmetry scattering ($m=0$), and Table I D for π-symmetry scattering ($m=1$)].

These basis sets have been tested for elastic e^--H_2 scattering in the static-exchange approximation and yield cross sections accurate to within a few percent for the impact energies considered here. We estimate that matrix elements calculcated by means of the approximate wave functions ψ^t_{klm} may be in error by as much as 10% owing to lack of convergence of the scattering basis sets. In this approach the Born part of the distorted-wave matrix element is treated exactly [since the kinetic-energy operator is not approximated in Eq. (33)], hence errors in our results due to basis set effects should decrease with increasing impact energy and partial-wave index.

Our approach to converging the single-center expansion of the electronic transition matrix element is to calculate in the distorted-wave approximation the partial-wave transition matrix elements up to where the Born approximation is valid, i.e.,

$$\langle \psi^{(-)}_{k_n lm} | U_{no} | \psi^{(+)}_{k_0 l'm} \rangle \simeq \langle \phi_{k_n lm} | U_{no} | \phi_{k_0 l'm} \rangle . \quad (53)$$

Contributions from higher partial-wave matrix elements are then included in the Born approximation. In this calculation we included the matrix elements for $l, l' \leq 6$, $m=0,1$ in the distorted-wave approximation. For higher partial waves, Born and distorted-wave matrix elements agree to within 1%. For excitation of the $b\ ^3\Sigma_u^+$ state (which occurs only via the exchange interaction) we also included Born matrix elements of U^{ex}_{no} for $l, l' \leq 5$, $m=2$. The contribution from these

matrix elements to the $b\ ^3\Sigma_u^+$ cross section is less than 5%, hence higher partial-wave matrix elements have been neglected. The differential cross section for excitation of the $b\ ^3\Sigma_u^+$ state was obtained by using Eqs. (18) and (19). We calculated differential cross section for excitation of the $B\ ^1\Sigma_u^+$ state using the j_t-basis representation according to Eq. (23). Convergence of this expansion to within 1% was obtained by including $j_t \leq 3$ and $m_t \leq 3$. For a $\Sigma \rightarrow \Sigma$ transition $m_t' = 0$. The contribution from high-angular-momentum scattering was included by the prescription given in Eqs. (25) and (26).

In general, the summation over final vibrational states includes both discrete and continuum states. The $b\ ^3\Sigma_u^+$ state is dissociative; hence all its vibrational states lie in the continuum. To obtain Franck-Condon factors for the transition $X\ ^1\Sigma_g^+ \rightarrow b\ ^3\Sigma_u^+$, we computed continuum vibrational wave functions for the $b\ ^3\Sigma_u^+$ state using the potential curves of Kolos and Wolniewicz[23] and approximated the ground-state vibrational level of the $X\ ^1\Sigma_g^+$ state by a harmonic-oscillator wave function. Our calculated Franck-Condon factors are in good agreement with the factors calculated by Rescigno *et al.*[2] For the $X\ ^1\Sigma_g^+ \rightarrow B\ ^1\Sigma_u^+$ transition we use the Franck-Condon factors calculated by Cartwright.[24] Adequate convergence of the sum over v_n was obtained by including only the Franck-Condon factors for transitions to discrete vibrational levels.

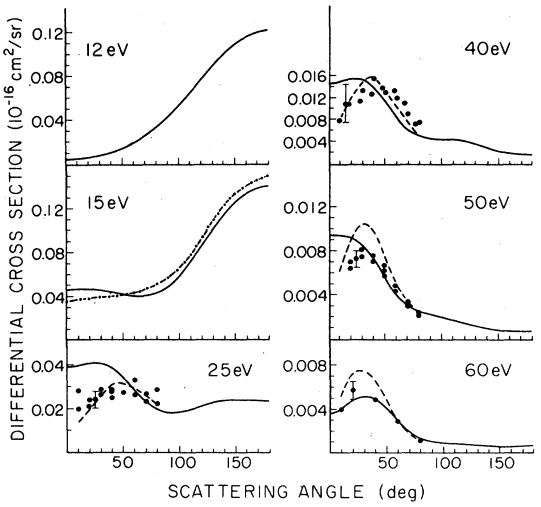

FIG. 1. Differential cross sections for excitation of the $^3\Sigma_u^+$ state at indicated electron impact energies; ——: DW results of this work; —·—·—: DW-RPA result from Ref. 2; — — — —: Born-Ochkur-Rudge results from Ref. 13; solid dots: relative experimental data from Ref. 13 normalized to our results.

Our differential cross section results (summed over final vibrational states) for excitation of the $b\ ^3\Sigma_u^+$ electronic state are given in Table I for impact energies from 12 to 60 eV. Six of these cross sections are shown in Fig. 1 by solid curves; the dashed curves show the Born-Ochkur-Rudge re-

TABLE I. Differential cross section for excitation of the $^3\Sigma_u^+$ state in units of 10^{-16} cm^2/sr.

Impact energy (eV)	12	15	20	25	30	40	50	60
Scattering angle (deg)	(10^{-2}) [a]	(10^{-2})	(10^{-2})	(10^{-2})	(10^{-2})	(10^{-3})	(10^{-3})	(10^{-3})
0	0.412	4.66	5.57	3.86	2.80	14.4	9.39	3.63
10	0.454	4.66	5.61	3.92	2.86	14.7	9.40	3.98
20	0.577	4.66	5.69	4.03	2.96	15.3	9.26	4.70
30	0.779	4.59	5.68	4.05	2.98	15.2	8.60	5.16
40	1.06	4.44	5.43	3.85	2.81	13.8	7.31	4.90
50	1.43	4.22	4.95	3.42	2.44	11.2	5.67	4.02
60	1.92	4.03	4.32	2.86	1.98	8.44	4.17	2.91
70	2.54	3.99	3.74	2.33	1.54	6.20	3.12	1.96
80	3.31	4.25	3.37	1.96	1.24	4.93	2.54	1.35
90	4.25	4.88	3.33	1.80	1.09	4.49	2.23	1.03
100	5.33	5.88	3.60	1.83	1.06	4.46	2.00	0.891
110	6.51	7.18	4.10	1.97	1.09	4.42	1.74	0.832
120	7.73	8.63	4.71	2.13	1.11	4.13	1.45	0.772
130	8.90	1.01	5.29	2.27	1.11	3.59	1.18	0.677
140	9.98	11.4	5.78	2.34	1.08	2.94	0.945	0.571
150	10.9	12.5	6.15	2.37	1.04	2.36	0.795	0.515
160	11.6	13.4	6.39	2.36	0.990	1.96	0.728	0.543
170	12.0	13.8	6.53	2.34	0.958	1.75	0.718	0.621
180	12.1	14.0	6.57	2.33	0.947	1.69	0.722	0.661

[a] The numbers in each column are to be multiplied by the factors in this row.

TABLE II. Integrated cross sections for excitation of the $b\,^3\Sigma_u^+$ state in units of 10^{-17}cm^2.

Impact energy (eV)	DW [a]	DW-RPA [b]	CC [c]	BR [d]	Experiment [e]
11	3.50			3.3 [f]	4.6±1.4
12	6.25			4.3 [f]	6.2±1.9
13	7.85	8.20	2.19	4.47	
15	8.30	8.89	2.80	4.18	
16	8.03	8.44	2.84	3.88	
18	6.81	7.0 [f]	2.7 [f]		
20	5.78	5.49	2.53	2.69	
22	4.53		2.3 [f]		
25	3.16		1.82	1.70	
30	1.95		1.26	1.10	
40	0.817		0.622	0.525	
50	0.402			0.287	
60	0.237			0.17 [f]	

[a] Results of this work.
[b] Results from Ref. 1.
[c] Two-state close-coupling results from Ref. 11.
[d] Born-Rudge results from Ref. 25.
[e] Experimental data from Ref. 12.
[f] Estimated by interpolation.

sults of Trajmar *et al.*[13]; the dash-dot-dash curve at 15 eV is the DW-RPA result of Rescigno *et al.*,[2] and the solid dots are the experimental results obtained by Trajmar *et al.*[13] normalized to our results at 40° for 50 and 60 eV and to the Born-Ochkur-Rudge results for 25 and 40 eV. Our integrated cross section results for excitation of the $b\,^3\Sigma_u^+$ state from 11 to 60 eV are given in Table II together with the DW-RPA results of Rescigno *et al.*, the two-state close-coupling results of Chung and Lin,[10] and Lee.[25] Below 11.8 eV the dissociation of H_2 by electron impact procedes purely by excitation of the $b\,^3\Sigma_u^+$ state; hence we have included Corrigan's experimental dissociation data at 11 and 12 eV impact energy in Table II.[12] These theoretical results are shown in Fig. 2, and Corrigan's dissociation data are shown up to 25 eV impact energy. Between 11.8 and 15.4 eV Corrigan's data essentially reflect the sum of all triplet-state excitation cross sections. Above 15.4 eV the reaction $e^- + H_2 \rightarrow H_2^+ + 2e^-$ also contributes. Corrigan's estimated experimental uncertainty is ±30%.[12] We estimate the uncertainty in our results for the $b\,^3\Sigma_u^+$ state due to numerical roundoff errors and the use of a discrete-basis-set representation of the distorted-wave potential at ±10% for total cross section and ±20% for the differential cross section.

Our distorted-wave differential cross sections summed over final vibrational states for excitation of the $B\,^1\Sigma_u^+$ state are given in Table III for impact energies from 15 to 60 eV. Conversion factors equal to $k_{v_2 q_{v_2 v_0}} / \sum_{v'} q_{v' v_0}$ for obtaining the cross sections for excitation of the $v' = 2$ vibrational sublevel at each energy are also given in Table III. Our differential cross sections for the excitation $X\,^1\Sigma_g^+(v=0) \rightarrow B\,^1\Sigma_u^+(v'=2)$ are shown in Fig. 3 and compared with the experimental data

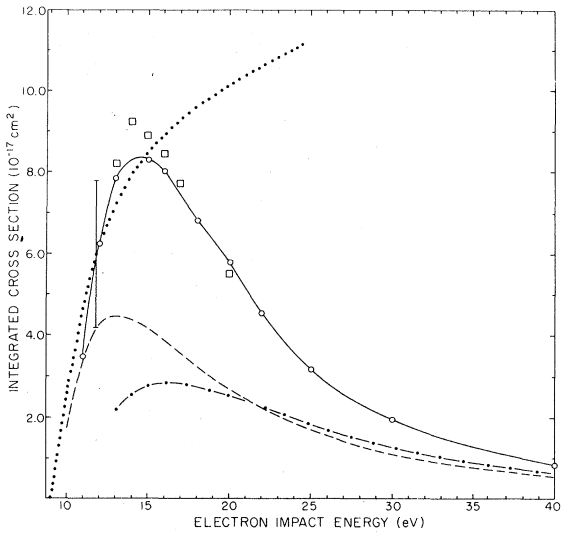

FIG. 2. Integrated cross section for excitation of the $b\,^3\Sigma_u^+$ state by electron impact; ——: DW results of this work, calculated points are indicated by open circles; open squares: DW-RPA results from Ref. 2; —∘—•—: two-state close-coupling results from Ref. 11; — — — —: Born-Rudge results from Ref. 25; ·····: experimental H_2 dissociation data from Ref. 12, error bar shows estimated uncertainty.

TABLE III. Differential cross section for excitation of the $B^1\Sigma_u^+$ state in units of 10^{-16} cm^2/sr.

Impact energy (eV)	15	20	25	30	40	50	60
Scattering angle (deg)	(10^{-3})	(10^{-3})	(10^{-3})	(10^{-3})	(10^{-3})	(10^{-3})	(10^{-3})
0	43.9	337	786	135	269	3950	5200
10	40.0	274	560	826	119	1270	1210
20	29.9	160	252	292	282	234	181
30	19.0	77.0	96.2	90.0	61.8	44.4	30.0
40	11.0	36.5	39.6	32.3	18.6	13.2	9.63
50	6.53	21.0	23.0	19.1	13.1	9.15	7.16
60	4.92	16.1	18.3	16.1	12.6	8.21	5.97
70	4.85	14.5	15.9	13.9	11.0	6.99	4.51
80	5.38	13.2	13.2	11.0	8.79	5.58	3.16
90	5.97	11.8	10.5	8.06	6.50	4.36	2.16
100	6.44	10.4	8.04	5.60	4.62	3.45	1.54
110	6.73	9.17	6.20	3.87	3.22	2.76	1.17
120	6.95	8.27	4.98	2.81	2.23	2.21	0.947
130	7.10	7.67	4.27	2.20	1.55	1.77	0.813
140	7.24	7.30	3.86	1.85	1.11	1.46	0.777
150	7.37	7.80	3.61	1.62	0.838	1.32	0.839
160	7.49	6.93	3.46	1.47	0.669	1.32	0.968
170	7.57	6.85	3.37	1.37	0.574	1.39	1.09
180	7.60	6.82	3.34	1.35	0.543	1.42	1.15
Conversion factor [a]	38.6	34.2	33.3	33.0	32.7	32.4	32.3

[a] Conversion factor for obtaining cross sections for the excitation $X^1\Sigma_g^+(v=0) \rightarrow B^1\Sigma_u^+(v=2)$ from DW entries in Tables III and IV.

of Srivastava and Jensen.[10] The solid curves show the distorted-wave approximation; the dashed curves show the first Born approximation for our choice of target wave functions. We assign the same error estimates for the $B\,^1\Sigma_u^+$ results as for the $b\,^3\Sigma_u^+$-state results. Table IV gives our integrated cross section results for excitation of the $B\,^1\Sigma_u^+$ state. Table IV compares our distorted-wave and Born results with the two-state close-coupling, Born-Ochkur, and Born results of Chung and Lin,[11] and with the experimental data of Srivastava and Jensen.[10] The theoretical results and experimental data are shown in Fig. 4.

IV. DISCUSSION AND CONCLUSIONS

We have demonstrated the utility of our discrete-basis-set method for obtaining electron-molecule continuum wave functions which can then be used in a distorted-wave-approximation calculation of electronic excitation by electron impact. Particular advantages of this method for treatment of inelastic scattering processes include: (a) the truncated distorted-wave potential V^t is expanded entirely in a square-integrable basis set and can be constructed by using standard molecular-bound-state computer codes, (b) the approximate continuum wave functions can be obtained at arbitrary scattering energies, and (c) these wave-functions satisfy the correct asymptotic scattering boundary conditions. Property (c) allows the treatment of scattering processes, such as the $X\,^1\Sigma_g^+ \rightarrow B\,^1\Sigma_u^+$ excitation process, where the transition potential has a long-range tail. Errors due to truncation of the distorted-wave potential could be investigated systematically by a generalization to multichannel scattering of the variational correction formula previously applied to elastic scattering.[6] In the present application we expect these errors are small since the basis sets used in this work give good results for elastic e^--H_2 scattering in the static-exchange approximation.[6]

Available theoretical and experimental differential cross sections for the $b\,^3\Sigma_u^+$ state are limited. As shown in Fig. 1 our results are in good agreement with the DW-RPA results of Rescigno *et al.* at 15-eV impact energy. The chief difference between our results and the Born-Ochkur-Rudge results of Trajmar *et al.*[13] occurs at small scattering angles where the latter drop off sharply, unlike our calculated cross sections which are roughly constant for scattering angles less than

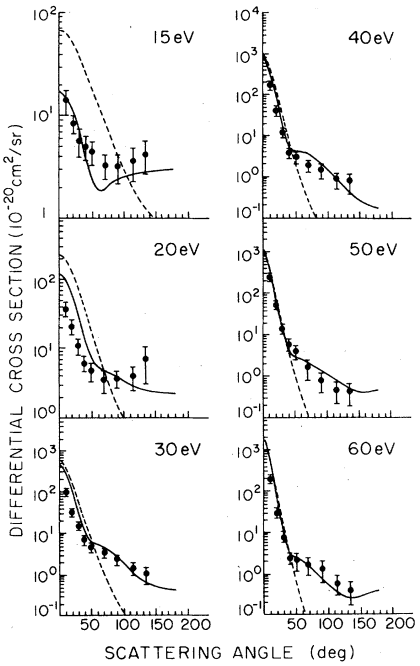

FIG. 3. Differential cross sections for excitation of the $B^1\Sigma_u^+(v'=2)$ state at indicated electron impact energies. The solid curves show the DW results of this work. The dashed curves show the Born results of this work. The solid dots with error bars show the experimental data of Ref. 10.

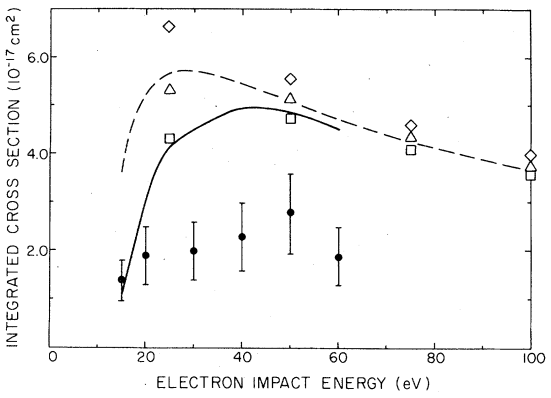

FIG. 4. Integrated cross section for excitation of the $B^1\Sigma_u^+$ state by electron impact. ——: DW result of this work; ----: Born result of this work; open squares: two-state close-coupling results from Ref. 11; open triangles: Born-Ochkur results from Ref. 11; open diamonds: Born results from Ref. 11; solid dots with error bars: experimental data from Ref. 10.

40°. Comparison of these results and the experimental angular distribution results of Trajmar *et al.*[13] at 25 and 40 eV is inconclusive owing to the large experimental error bars (shown in Fig. 1) and limited range of scattering angles. The agreement both between the DW and Born-Ochkur-Rudge results and between theory and experiment is quite good at 50 and 60 eV.

The good agreement between our DW results for the $b\,^3\Sigma_u^+$ state and the DW-RPA is an important check on the numerical accuracy of these calculations as well as a verification of the validity of the present choice for the transition potential. In contrast to our approach Rescigno *et al.* expanded the continuum wave functions in a set of Gaussian functions. This representation, which does not lead to the correct asymptotic form, seems to be adequate for singlet-triplet excitations owing to the short-range nature of the exchange interaction. Another difference between their approach and ours is that in their calculation the averaging over target orientation was carried out numerically, whereas in ours this averaging is treated analytically via a single-center expansion of the scattering amplitude.

TABLE IV. Integrated cross section for excitation of the $B^1\Sigma_u^+$ state in units of 10^{-17}cm^2.

Impact energy (eV)	DW [a]	Born I [b]	CC [c]	BO [d]	Born II [e]	Experiment [f]
15	1.05	3.60				1.4±0.4
20	3.09	5.23				1.9±0.6
25	4.12	5.64	4.31	5.31	6.66	
30	4.46	5.69				2.0±0.6
40	4.93	5.43				2.3±0.7
50	4.84	5.06	4.71	5.14	5.55	2.8±0.8
60	4.49	4.70				1.9±0.6

[a] Results of this work.
[b] Born results of this work.
[c] Two-state close-coupling results from Ref. 11.
[d] Born-Ochkur results from Ref. 11.
[e] Results from Ref. 11.
[f] Experimental data from Ref. 10.

Figure 2 shows that at 20 eV our DW integrated cross section for the $b\,^3\Sigma_u^+$ state is a factor of 2 larger than the two-state close-coupling results of Chung and Lin.[11] This difference reflects in part the sensitivity of the exchange excitation process to approximations in the scattering wave function. Another part of this difference is due to the use of different H_2 excited-state wave functions. Chung and Lin[11] use an SCF wave function for the excited state, while in this work the excited σ_u orbital is calculated in the field of the ground state σ_g orbital. Since the Born-Rudge approximation uses plane-wave functions, the good agreement of this approximation with the two-state close-coupling result above 20 eV appears to be fortuitous.

In order to compare with Corrigan's data we have obtained DW results down to 11-eV impact energy. The distorted-wave model is generally believed to break down in the near-threshold region because channel coupling and resonance effects are expected to be large. There is a resonance in this cross section in the 10-eV region due to the $^2\Sigma_g$ state of H_2^-. However, experimental data indicate that the peak contribution from this resonance is about 1×10^{-17} cm^2 or about 20% of the nonresonance contribution.[26] Moreover, the accuracy of the DW approximation near threshold is of practical interest for electron-molecule scattering since more accurate methods are currently not available for larger systems. Figure 2 shows that the DW results and Corrigan's data in fairly good agreement at 11 and 12 eV, where dissociation occurs only via the $b\,^3\Sigma_u^+$. However, it would be premature to assess the reliability of the DW method near threshold based on this agreement.

At 30-eV impact energy and above, our DW differential cross sections for excitation of the $B\,^1\Sigma_u^+(v'=2)$ state are in good qualitative agreement with the data of Srivastava and Jensen.[10] As shown in Fig. 3, the chief discrepancy occurs at small scattering angles where the DW results are about a factor of 2 larger than experiment. Since the scattering is strongly forward peaked this leads to about a factor-of-2 difference in the integrated cross sections as shown in Fig. 4. Srivastava and Jensen[10] obtain the experimental integrated cross section summed over v' from their data by applying the Franck-Condon principle. As a check on the consistency of their treatment and ours, we note that the values they obtain for $\sigma(v'=2)/\sigma(\text{total})$ agree with the conversion factors given in Table III to within 10%.

Figure 3 shows that the BA differential cross section converges rapidly to the DW result with increase in impact energy at small scattering angles ($<40°$), while it significantly underestimates the cross section at large scattering angles. The good agreement between our BA and DW integrated cross sections above 30 eV is due to the small contribution to the total scattered flux from large-angle scattering. Thus this excitation process is dominated by the long-range dipole transition potential.

The difference between our BA integrated cross section and the Born result of Chung and Lin[11] indicates the effect of using different final-target-state approximate wave functions in the two calculations. At 50-eV impact energy and above, this difference is less than 10% of the integrated cross section, and the DW and two-state close-coupling results are in good agreement. The lack of convergence of the theoretical and experimental integrated cross sections with increase in impact energy is puzzling in light of the good agreement between the various theoretical results by 50 eV. In this regard it would be of interest to extend the experimental results to higher impact energy.

ACKNOWLEDGMENTS

We acknowledge the support of the National Science Foundation through Grant No. CHE76-05157. We thank Dr. S. Trajmar for helpful discussions about the experimental data shown in this work, and Dr. D. C. Cartwright for the use of his unpublished Franck-Condon factors for the $X\,^1\Sigma_g^+\rightarrow B\,^1\Sigma_u^+$ transition. We also thank D. A. Levin and Dr. T. N. Rescigno for helpful discussions. We also acknowledge support by an Institutional Grant from the Department of Energy EY-76-G03-1305.

APPENDIX

This appendix outlines the derivation of closed-form expressions for the j_t-basis coefficients $B^{j_t(\mathrm{BA})}_{m_t m_t'}(\hat{\Omega})$ assuming the target orbitals are expanded in terms of Cartesian Gaussians of the form

$$\mu^{\alpha\vec{A}}_{lmn}(\mathbf{r}) = N_{lmn}(x-A_x)^l(y-a_y)^m(z-A\ )^n e^{-\alpha|\vec{r}-\vec{A}|^2}, \tag{A1}$$

where N_{lmn} is a normalization coefficient. In this case the scattering amplitude is given by a sum of free-free Coulomb integrals of the form

$$F=\langle e^{-\vec{k}'\cdot\vec{r}_1}\,\mu^{\alpha\vec{A}}_{l'm'n'}(\vec{r}_2)\,|v|\,e^{i\vec{k}\cdot\vec{r}_1}\mu^{\beta\vec{B}}_{l''m''n''}(\vec{r}_2)\rangle\,. \tag{A2}$$

Evaluation of this integral in the body-fixed frame leads to the general expression[27]

$$F = N_{l'm'n'} N_{l''m''n''} A(\alpha, \beta, |\vec{A} - \vec{B}|, q) \times e^{-i\vec{q}\cdot\vec{R}_p} \sum_{i'j'k'}^{l'm'n'} \sum_{i''j''k''}^{l''m''n''} C_{ijk} \times H_i\left(\frac{-q_x}{2(\alpha+\beta)^{1/2}}\right) H_j\left(\frac{-q_y}{2(\alpha+\beta)^{1/2}}\right) H_k\left(\frac{-q_z}{(\alpha+\beta)^{1/2}}\right), \tag{A3a}$$

where

$$A(\alpha, \beta, |\vec{A} - \vec{B}|, q) = \frac{4\pi^{5/2}}{q^2} \exp[-(\alpha\beta/\alpha+\beta)|\vec{A} - \vec{B}|^2] \times \exp[-q^{2/4(\alpha+\beta)}] \tag{A3b}$$

$$C_{ijk} = C^{l'm'n'}_{i'j'k'} C^{l''m''n''}_{i''j''k''} \times i^{-i+j+k} [(\alpha+\beta)^{(i+j+k)/2} 2^{i+j+k}]^{-1}, \tag{A3c}$$

$$i = i' + i'', \quad j = j' + j'', \quad k = k' + k'', \tag{A3d}$$

$$C^{l'm'n'}_{i'j'k'} = \binom{l'}{i'}\binom{m'}{j'}\binom{n'}{k'} (P_x - A_x)^{l'-i'} \times (P_y - A_y)^{m'-j'} (P_z - A_z)^{n'-k'}, \tag{A3e}$$

$$\binom{l'}{i'} = \frac{l'!}{i'!(l'-i')!}, \tag{A3f}$$

$$\vec{R}_p = \vec{P} = (\alpha\vec{A} + \beta\vec{B})/(\alpha+\beta), \tag{A3g}$$

$$\vec{q} = \vec{k}' - \vec{k}, \tag{A3h}$$

and H_i is an Hermite polynomial. To evaluate the integral on the right-hand side of Eq. (22), we transform the expression for F to the coordinates of the laboratory frame. Calculation of the coefficients $B^{j_t}_{m_t m_t'}(\hat{\Omega}')$ then essentially involves evaluation of integral

$$F^{j_t}_{m_t m_t'}(q') = \frac{2j_t+1}{8\pi^2} \int d\hat{R}'\, D^{(j_t)}_{m_t m_t'}(\hat{R}') F(\hat{q}', \hat{R}'). \tag{A4}$$

To express F in the laboratory frame coordinates, we first note that the product of Hermite polynomials occurring in Eq. (A3a) may be expanded in a finite series of spherical harmonics:

$$H_i H_j H_k = \sum_{sm_s} f_{sm_s}\left(\frac{q}{2(\alpha+\beta)^{1/2}}\right) Y_{sm_s}(\hat{q}), \tag{A5a}$$

where

$$s \le i+j+k = i'+i''+j'+j''+k'+k''. \tag{A5b}$$

Using Eq. (A5a) we can rewrite Eq. (A3a) in the form

$$F = \sum_{\substack{i'j'k' \\ i''j''k''}} \sum_{sm_s} S^{ijk}_{sm_s} Y_{sm_s}(\hat{q}) e^{-i\vec{R}_p\cdot\vec{q}} \tag{A6a}$$

where

$$S^{ijk}_{sm_s} = N_{l'm'n'} N_{l''m''n''} A(\alpha, \beta, |\vec{A} - \vec{B}|, q) C_{ijk} f_{sm_s} \tag{A6b}$$

transforms as a scalar under rotations. The factor $e^{i\vec{q}\cdot\vec{R}_p}$ is also a scalar, and hence

$$e^{-i\vec{q}\cdot\vec{R}_p} = e^{-i\vec{q}'\cdot\vec{R}_p'} \tag{A7}$$

(the primes indicate laboratory-frame coordinates). From the properties of spherical harmonics under rotations we have

$$Y_{sm_s}(\vec{q}) = \sum_{m''} D^{(s)}_{m'',m_s}(\hat{R}') Y_{sm''}(\hat{q}'). \tag{A8}$$

There is a one-to-one correspondence between the target orientation angles, denoted by $\hat{R}'$, and the unit vector $\hat{R}_p'$. For a linear target molecule we may set $\hat{R}_p' = \hat{R}'$ without loss of generality. The expression for F in laboratory frame is then of the form

$$F(\hat{q}', \hat{R}') = \sum_{\substack{i'j'k' \\ i''j''k''}} \sum_{sm_s} S^{ijk}_{sm_s} \Phi^{sm_s}(\hat{q}', \hat{R}'), \tag{A9a}$$

where

$$\Phi^{sm_s}(\hat{q}', \hat{R}') = \sum_{m''} D^{(s)}_{m'',m_s}(\hat{R}') Y_{sm_s''}(\hat{q}') \exp[-i(qR_p)\hat{q}'\cdot\hat{R}']. \tag{A9b}$$

Similarly,

$$F^{j_t}_{m_t,m_t'}(\hat{q}') = \sum_{\substack{i'j'k' \\ i''j''k''}} \sum_{sm_s} S^{ijk}_{sm_s} \Phi^{sm_s}_{j_t m_t m_t'}(\hat{q}'), \tag{A10a}$$

where we define

$$\Phi^{sm_s}_{j_t m_t m_t'}(\hat{q}') = \frac{2j_t+1}{8\pi^2} \int d\hat{R}'\, D^{(j_t)}_{m_t,m_t'}(\hat{R}') \Phi^{sm_s}(\hat{R}', \hat{q}'). \tag{A10b}$$

Introducing the single-center expansion

$$e^{-i\vec{q}'\cdot\vec{R}_p'} = 4\pi \sum_{LM} i^L j_L(-qR_p) Y_{LM}(\hat{q}') Y^*_{LM}(\hat{R}') \tag{A11}$$

and using the relation

$$Y^*_{LM}(\hat{R}') = (2L+1/4\pi)^{1/2} D^{(L)}_{M0}(\hat{R}'), \tag{A12}$$

$\Phi^{sm_s}(\hat{q}, \hat{R}')$ can be written as follows:

$$\Phi^{sm_s}(q', R') = \sum_{LMm''} i^L [4\pi(2L+1)]^{1/2} j_L(-R_p q) \times D^{(s)}_{m'',m_s}(\hat{R}') D^{(L)}_{M0}(\hat{R}') Y_{sm''}(\hat{q}') Y_{LM}(\hat{q}'). \tag{A13}$$

Substituting Eq. (A13) into Eq. (A10b) and applying

the completeness properties of rotational and spherical harmonics, we obtain

$$\Phi^{sm_s}_{j_t m_t m'_t}(q') = [(2s+1)(2j_t+1)]^{1/2} \sum_L i^L \frac{2L+1}{2j_t+1} (Ls0m_s | j_t m'_t)(L200 | j_t 0) Y_{j_t m_t}(\hat{q}') . \tag{A14}$$

Expressions for the coefficients $B^{j_t(\mathrm{BA})}_{m_t m'_t}(\hat{\Omega}')$ follow directly.

---

*Contribution No. 5930.

[1]B. H. Bransden and M. R. C. McDowell, Phys. Rep. 46, 249 (1978).
[2]T. N. Rescigno, C. W. McCurdy, Jr., V. McKoy, and C. F. Bender, Phys. Rev. A 13, 216 (1976).
[3]T. N. Rescigno, C. W. McCurdy, Jr., and V. McKoy, J. Phys. B 7, 2396 (1974).
[4]G. Csanak, H. S. Taylor, and R. Yaris, Phys. Rev. A 3, 1322 (1971); G. Csanak, H. S. Taylor, and D. N. Tripathy, J. Phys. B 6, 2040 (1973).
[5]L. D. Thomas, G. Csanak, H. S. Taylor, and B. S. Yarlagadda, J. Phys. B 7, 1719 (1974).
[6]A. W. Fliflet and V. McKoy, Phys. Rev. A 18, 2107 (1978).
[7]T. N. Rescigno, C. W. McCurdy, Jr., and V. McKoy, Chem. Phys. Lett. 27, 401 (1974); Phys. Rev. A 10, 2240 (1974); 11, 825 (1975).
[8]U. Fano and D. Dill, Phys. Rev. A 6, 185 (1972).
[9]J. Siegel, D. Dill, and J. L. Dehmer, Phys. Rev. A 17, 2106 (1978).
[10]S. K. Srivastava and S. Jensen, J. Phys. B 10, 3341 (1977).
[11]S. Chung and C. C. Lin, Phys. Rev. A 17, 1874 (1978).
[12]S. J. B. Corrigan, J. Chem. Phys. 43, 4381 (1965).
[13]S. Trajmar, D. C. Cartwright, J. K. Rice, R. T. Brinkmann, and A. Kuppermann, J. Chem. Phys. 49, 5464 (1968).
[14]J. R. Taylor, *Scattering Theory* (Wiley, New York, 1972), p. 418.
[15]C. W. McCurdy, Jr., T. N. Rescigno, D. L. Yeager, and V. McKoy, *Modern Theoretical Chemistry 3*, edited by H. F. Schaefer III (Plenum, New York, 1977), p. 339.
[16]H. P. Kelly, Phys. Rev. 136, B896 (1964).
[17]A. R. Edmonds, *Angular Momentum in Quantum Mechanics* (Princeton University, Princeton, N. J., 1960).
[18]A. Temkin, K. V. Vasavada, E. S. Chang, and A. Silverman, Phys. Rev. 186, 57 (1969).
[19]D. M. Chase, Phys. Rev. 104, 838 (1956).
[20]R. G. Newton, *Scattering Theory of Waves and Particles* (McGraw-Hill, New York, 1966), p. 191.
[21]A. W. Fliflet and V. McKoy, Phys. Rev. A 18, 1048 (1978).
[22]W. J. Hunt and W. A. Goddard III, Chem. Phys. Lett. 3, 414 (1969); 24, 464 (1974).
[23]W. Kolos and L. Wolniewicz, J. Chem. Phys. 43, 2429 (1965); 48, 3672 (1968).
[24]S. Trajmar (private communication).
[25]S. Chung, C. C. Lin, and E. T. P. Lee, Phys. Rev. A 12, 1340 (1975).
[26]G. J. Schulz, Rev. Mod. Phys. 45, 378 (1973).
[27]D. K. Watson and V. McKoy, Phys. Rev. A 20, 1474 (1979).